

Supplementary Figure 1. Epithelial NELF-B-deficient mice show normal crypt architecture and do not spontaneously develop colitis

(A and B) qPCR (A) and immunoblotting (B) analysis of *Nelfb* expression in colon tissues from *Nelfb*^{+/+}Villin-Cre and *Nelfb*^{fl/fl}Villin-Cre mice (n = 3-7).

(C) Immunoblotting analysis of NELF-E in colon tissues from *Nelfb*^{+/+}Villin-Cre and *Nelfb*^{fl/fl}Villin-Cre mice (n = 3).

(D) H&E and Alcian Blue (AB) staining analysis of morphologies of intestinal sections from *Nelfb*^{+/+}Villin-Cre and *Nelfb*^{fl/fl}Villin-Cre mice (n = 5-10). Scale bars, 50 μ m.

(E) Immunohistochemical analysis of Ki-67 protein levels in intestinal sections of *Nelfb*^{+/+}Villin-Cre and *Nelfb*^{fl/fl}Villin-Cre mice (n = 4). Scale bars, 50 μ m.

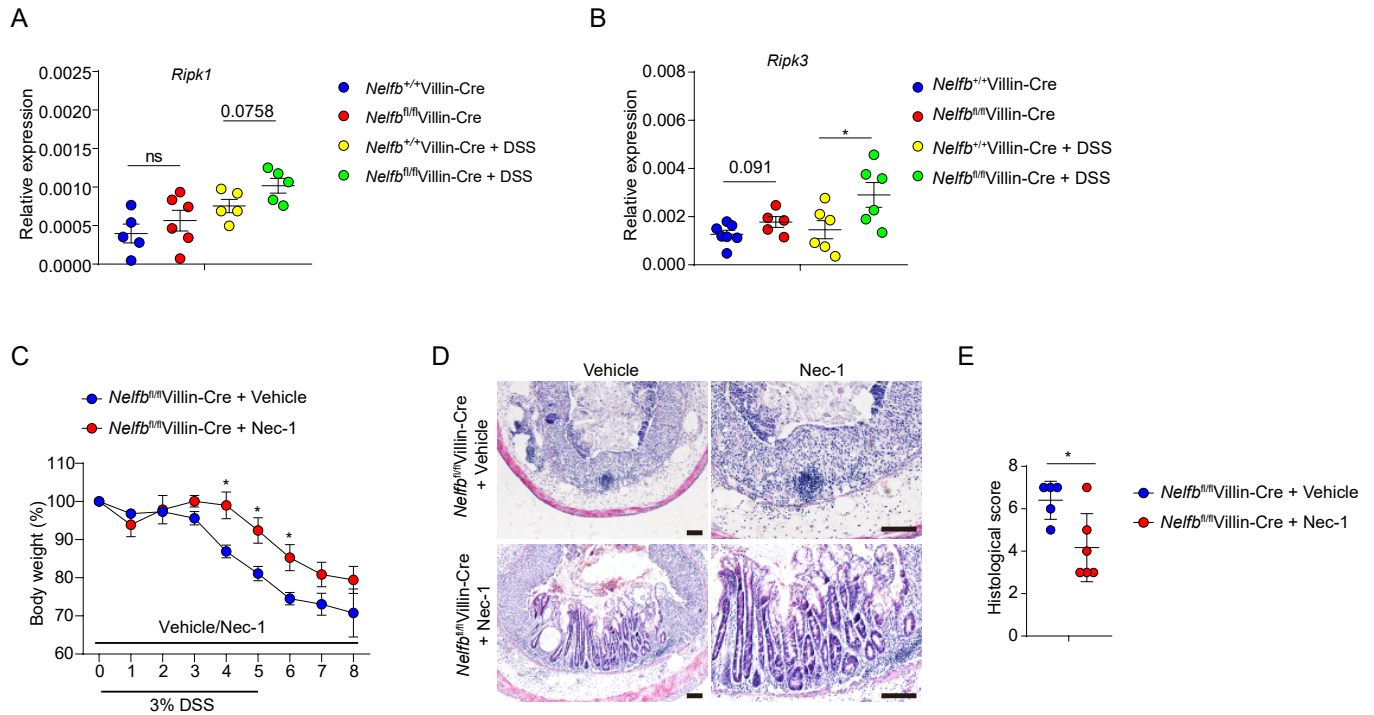
(F) Organoids of small intestine and colon from *Nelfb*^{+/+}Villin-Cre and *Nelfb*^{fl/fl}Villin-Cre mice visualized by light microscopy (n = 3). Circularities are calculated (right panel). Scale bars, 50 μ m.

(G-I) Body weight (G), H&E staining (H) and histological scores (I) of *Nelfb*^{fl/fl}Villin-Cre mice and littermate controls (*Nelfb*^{+/+}Villin-Cre) after DSS treatment (n = 4). Scale bar, 50 μ m.

(J) The experimental scheme for the procedure of intestinal permeability analysis.

(K) Intestinal permeability analysis of *Nelfb*^{+/+}Villin-Cre and *Nelfb*^{fl/fl}Villin-Cre mice under homeostasis condition (n = 8-9).

All data are shown as mean \pm SEM. Student's *t* test was performed; **p \leq 0.01; ns, not significant (p > 0.05).



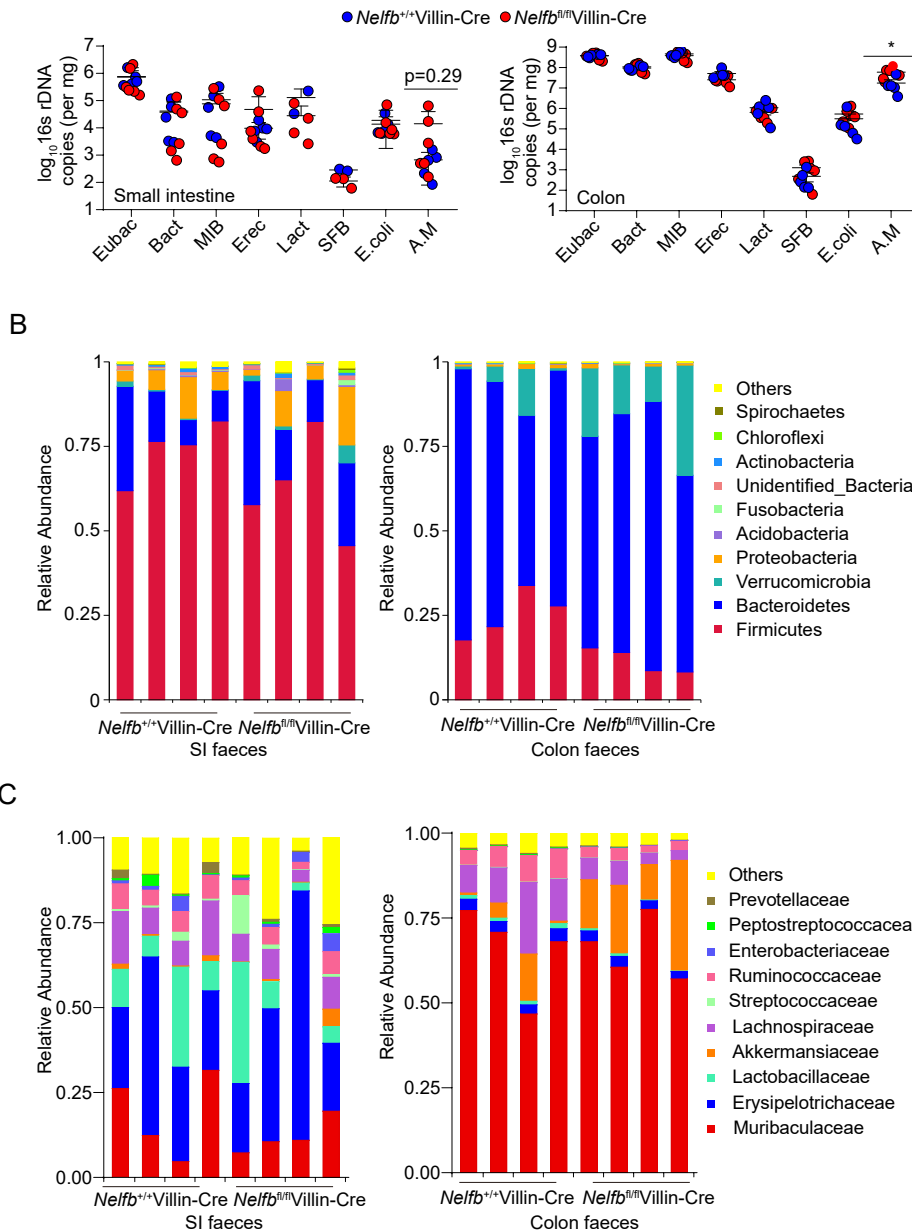
Supplementary Figure 2. Epithelial NELF inhibits IEC necroptosis

(A and B) qPCR analysis of the expression of *Ripk1* (A) and *Ripk3* (B) in *Nelfb*^{+/+}Villin-Cre and *Nelfb*^{fl/fl}Villin-Cre mice with or without DSS treatment (n = 5-7).

(C) Body weight of *Nelfb*^{fl/fl}Villin-Cre mice with or without necrostatin-1 stimulation after DSS treatment (n = 5-6).

(D and E) H&E staining (D) and histological scores (E) (n = 5-6) of colon sections from DSS treated mice as in (C) at day 8. Scale bars, 50 μ m.

All data are shown as mean \pm SEM. Student's *t* test was performed; **p* \leq 0.05; ns, not significant (*p*>0.05).

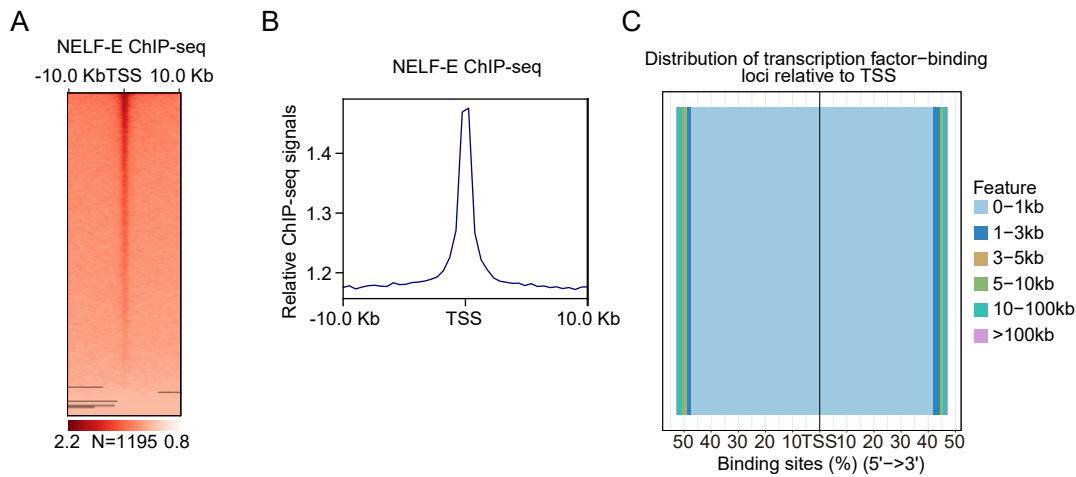


Supplementary Figure 3. Loss of epithelial NELF-B results in mild microbial changes in gut

(A) The abundance of microbiota in small intestine and colon of *Nelfb*^{+/+}Villin-Cre and *Nelfb*^{fl/fl}Villin-Cre mice was analyzed by qPCR analysis of 16S rDNA gene copy number (n = 6). Eubac, Eubacteria; Bact, *Bacteroides* spp.; MIB, mouse intestinal *Bacteroides*; Erec, *Eubaterium rectale/Clostridium coccoides*; Lact, *lactobacillus* sp.; SFB, segmented filamentous bacteria.

(B and C) 16S rDNA sequencing analysis of commensal diversity at the phylum level (B) and family level (C) in small intestine and colon of *Nelfb*^{+/+}Villin-Cre and *Nelfb*^{fl/fl}Villin-Cre littermate mice under homeostasis condition (n = 4).

All data are shown as mean \pm SEM. Student's *t* test was performed; * $p \leq 0.05$; ns, not significant ($p > 0.05$).

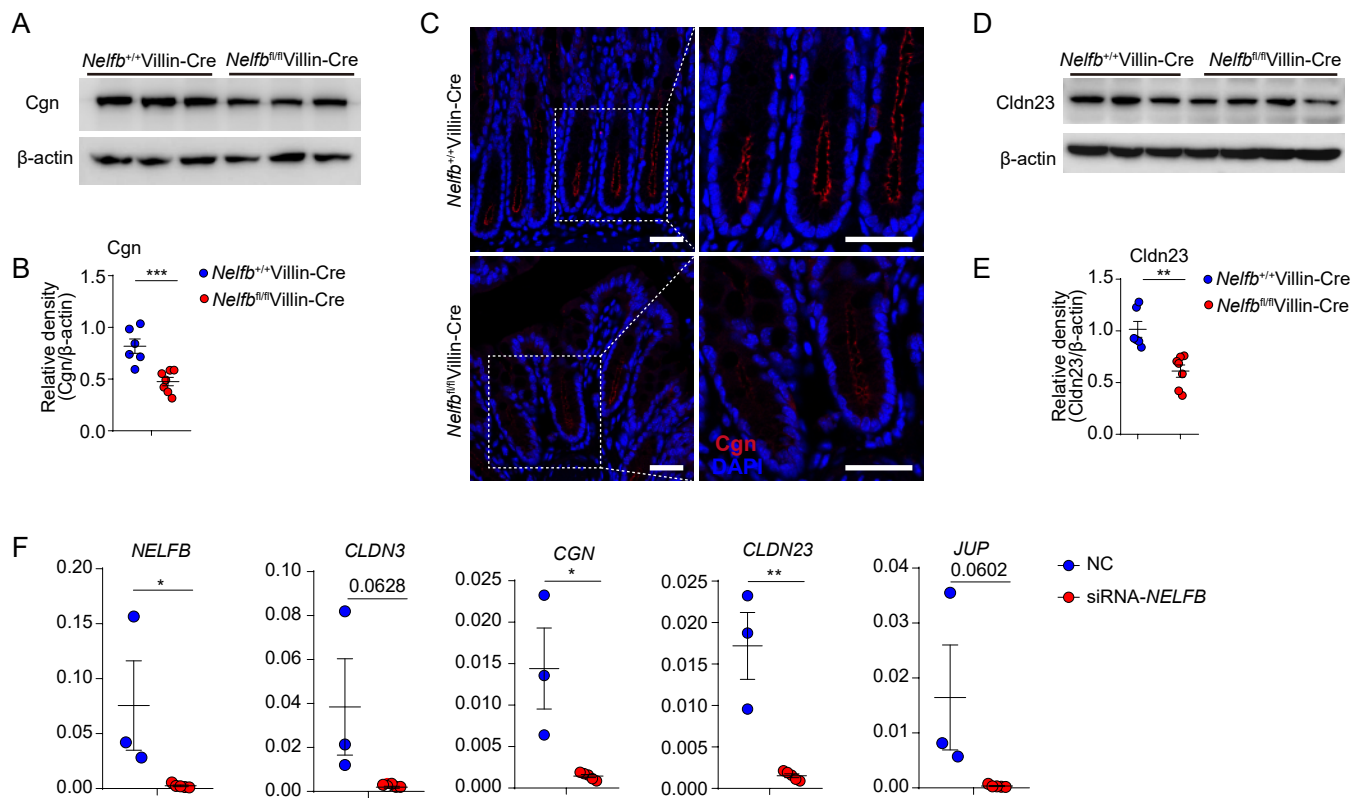


Supplementary Figure 4. ChIP-seq analysis results for NELF-B marks in colonic IECs

(A) Heat map of NELF-E ChIP-seq signals around TSS regions for colonic IEC-expressed genes in *Nelfb*^{+/+}Villin-Cre mice at steady state. Each row indicates one gene sorted by the peak heights in *Nelfb*^{+/+}Villin-Cre mice. The signals were normalized to input signals. The number of peaks in the whole genome is shown at the bottom.

(B) Relative NELF-E ChIP-seq signals around TSS regions as (A) shown.

(C) Distribution of NELF-E ChIP-seq peaks around transcription factor-binding loci relative to TSS.



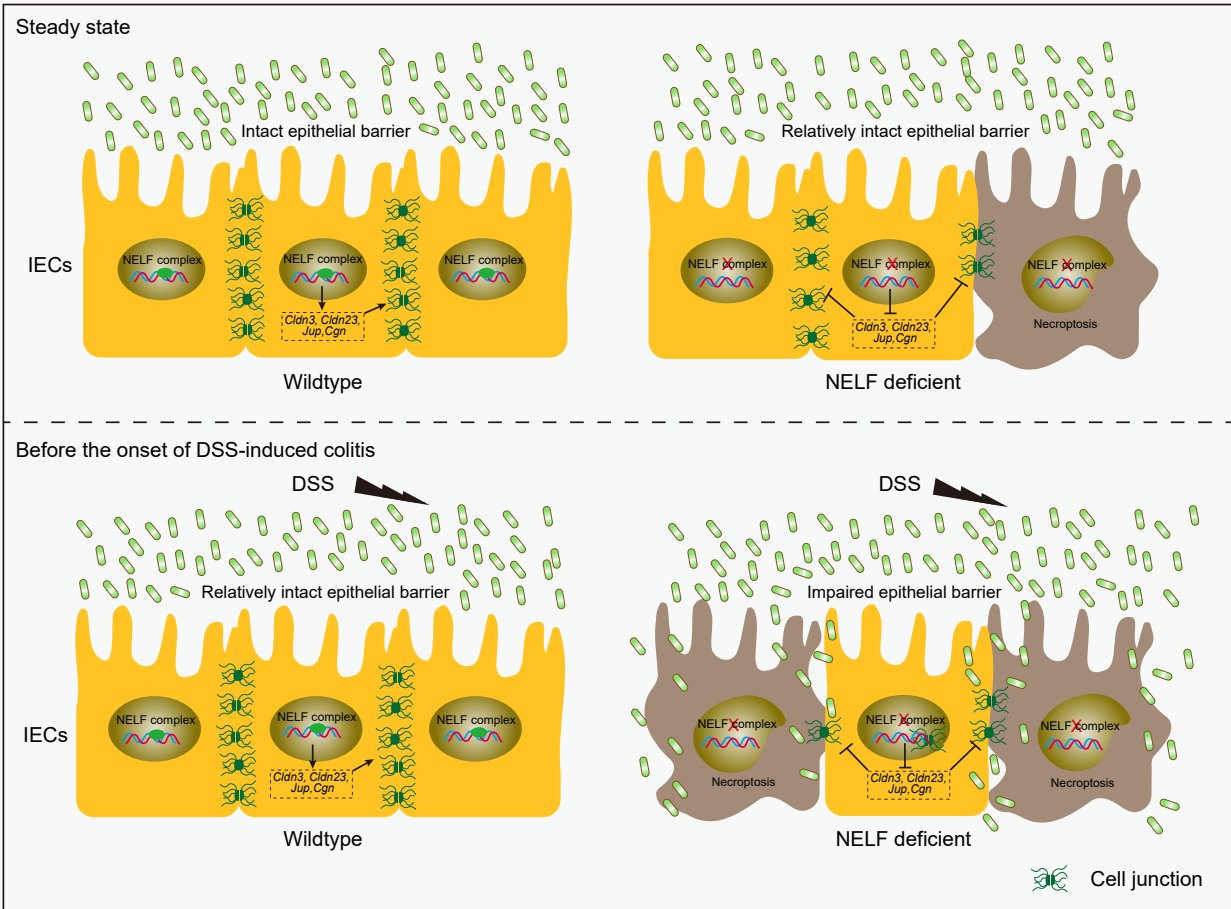
Supplementary Figure 5. Epithelial NELF promotes the expression of a subset of cell junction related genes

(A-C) Immunoblotting analysis (A), quantification (B) and immunofluorescent (C) analysis of Cgn expression in *Nelfb*^{+/+}Villin-Cre and *Nelfb*^{fl/fl}Villin-Cre mice (n = 6-7).

(D and E) Immunoblotting analysis (D) and quantification (E) analysis of Cldn23 expression in *Nelfb*^{+/+}Villin-Cre and *Nelfb*^{fl/fl}Villin-Cre mice (n = 6-7).

(F) qPCR analysis of cell junction-related genes expression in LS174T cells after siRNA against *NELFB*.

All data are shown as mean ± SEM. Student's t test was performed; *p ≤ 0.05, **p ≤ 0.01, ***p ≤ 0.001, ****p ≤ 0.0001; ns, not significant (p>0.05).



Supplementary Figure 6. Epithelial NELF maintains intestinal barrier function to repress colitis

A working model for epithelial NELF maintaining intestinal barrier function. Under steady state, genetic deletion of NELF complex in IECs results in reduction of genes associated with junctional integrity (such as *Cldn3* and *Cldn23*) and increased IEC necroptosis without significantly affecting epithelial barrier integrity in mice. However, upon DSS treatment, loss of epithelial NELF complex leads to reduction of genes associated with junctional integrity, impaired epithelial barrier characterized by increased permeability, bacterial invasion, and epithelial necroptosis before the onset of colitis, and consequently increased susceptibility to intestinal inflammation.

Supplementary Table 1: Primers used in this study

Primer sequences for regular qPCR		
Gene	Forward Primer	Reverse Primer
<i>Nelfb</i>	TGAGGCTTCTCCTCCACTT	GGTCTAACTGCTCCAACCTTCTC
<i>Cldn3</i>	CACCCACCAAGATCCTCTATTC	TTCATCGACTGCTGGTAGTG
<i>Cldn23</i>	TCTGTGTTGAGCTTGTGAGC	AGGTATCTCGGGAACAGGACA
<i>Jup</i>	CTGTTTGACTCCCACCACCT	CGCATGCCCTTACTTCCTC
<i>Cgn</i>	ACAAAAGACCCTCCTTATGGCTT	AGAGGCAAACCATCCCCAT
<i>Retnlb</i>	TCAGTCGTCAAGAGCCTAAGA	CATAGCCACAAGCACATCCA
<i>Ang4</i>	ACTCTGGCTCAGAATGAAAGGT	GACATCTTTGCAAGGCGAGG
<i>Itln1</i>	GCTGAAGAGAACCTGGACAC	GGTCTGGTAGATGACACCATTTC
<i>Spink4</i>	ACATGGCTGAGCTTCCAAA	AGCATTGGCCATCCTTCAT
<i>Mptx1</i>	ACAGCATCTTCTCCTACAACAC	GACTCCCAGTTCACACAGATAC
<i>Tgm3</i>	GTCTCCCCACACCATCTCTGT	CGTTTTGGATCTGTAAAGCACTCA
<i>Slc37a2</i>	GGAATGGTGCTAAGTGGCCT	ATGAATGACAGGCCCCAGTG
<i>Fabp6</i>	GTGAAGATGGAGGGTGGCAA	CGCTCATAGGTCACATCCCC
<i>Cyp3a44</i>	TTGGTCCTGCTGGCAATCAT	GCCCAGGAATCCCCGTGTTTC
<i>Gm20605</i>	CGAGCTTTTTGGGGACCTGA	CAACATCCTGCGACTGGTGA
<i>Ripk1</i>	CCACTTCAGCACCGAACTCC	CTTCTCCAGCAGGTCACTGG
<i>Ripk3</i>	GCCTTCCTCTCAGTCCACAC	ACGCACCAGTAGGCCATAAC
<i>Human NELFB</i>	GTATTCGATGAGCTGCGGGA	TTTCTCCGGAACCTTGGGC
<i>Human CLDN3</i>	GTCTAAGGGACAGACGCAGG	AAGTATTGGCGGTCACCCAG
<i>Human CGN</i>	CCCGGCTAGGGACTCCTC	CTGGCTCTGTGATGAAGCGA
<i>Human CLDN23</i>	ACTCCGACCTCTAGACGCTT	CAAGTGTCCGGGTTCCTCACT
<i>Human JUP</i>	GCCTCGTCGATACTACCTGC	GGTGTATGTCTGCTGCCACT
Eubacteria (Universal)	ACTCCTACGGGAGGCAGCAGT	ATTACCGCGGCTGCTGGC
<i>Bacteroides</i> (Bact)	GGTTCTGAGAGGAGGTCCC	CTGCCTCCCGTAGGAGT
Mouse Intestinal <i>Bacteroides</i> (MIB)	CCAGCAGCCGCGGTAATA	CGCATTCCGCATACTTCTC
<i>Lactobacillus/Enterococcus</i> Group (Lact)	AGCAGTAGGGAATCTTCC	CACCGCTACACATGGA
<i>Eubacterium rectale/ Clostridium coccooides</i> group (Erec)	ACTCCTACGGGAGGCAGC	GCTTCTTAGTCAGGTACCGTCA
Segmented filamentous bacteria (SFB)	GACGCTGAGGCATGAGAGCA	GACGGCACGGATTGTTATTC
<i>E. coli</i>	CATGCCGCGTGTATGAAGAA	CGGGTAACGTCAATGAGCAAA
<i>A. muciniphila</i>	CAGCACGTGAAGGTGGGGAC	CCTTGCGGTTGGCTTCAGAT
Primer sequences for ChIP assays		
Gene	Forward Primer	Reverse Primer
<i>Cldn3</i> TSS	CCTCCTCCTCTAGGCACCAA	GGCTTTGGAGACTGGCTTCT
<i>Cldn23</i> TSS	CGAAACCAGCTCCGAGTCC	CCACCCGGTAGGGTTTGG
<i>Cgn</i> TSS	TAGCTTAGCGCCAGAGCATC	GATGAAGGGCAGAAAGGGCT
<i>Jup</i> TSS	CAGCCTGACTATCCCATCGAG	GAGCGCATAAACAGAGGCGG
<i>Jun</i> TSS	CGTCTGTCTGTCTGTCTGCC	GCTCAGGCTGGATAAGGACTC
<i>Hbb</i> TSS	CAGGGAGAAATATGCTTGTCATCA	GTGAGCAGATTGGCCCTTACC